Fracture Decoupling Experiment Phase II

Anastasia Stroujkova, Jessie Bonner, and Mark Leidig
Weston Geophysical Corp.

INTRODUCTION

The Former Soviet Union (FSU) practiced detonating multiple nuclear tests in the same or similar tunnel location. It has been observed that the seismic amplitudes of the "repeat nuclear test" are significantly decreased, when compared to a "first nuclear test" of the same yield (e.g. Sokolova, 2008). In addition, several calibration chemical explosions conducted at the Semipalatinsk Test Site (STS) confirm that fracture decoupling reduces the amplitudes of the secondary shots (e.g. Knowles, 2006). The decreased seismic amplitudes reduce the detection/identification thresholds and seismically estimated yield of a "repeat nuclear explosion" and could act as a "decoupling" mechanism.

The objective of the proposed research is to conduct a seismic field experiment to:

a) Define the physics responsible for causing seismic amplitude reductions and
b) Quantify the phenomena in terms of a "decoupling factor" as a function of frequency.

In order to quantify the degree of the amplitude reduction and to evaluate possibilities of concealing nuclear tests, Weston Geophysical Corp. (WGC) in cooperation with Columbia University's Lamont Doherty Earth Observatory (LDEO) conducted a multi-phase field experiment near Groton, NH. The objective of this project is to conduct a series of co-located explosion pairs ranging from 500 to 2000 lbs to extensively fractured granitic emplacement media in order to achieve project's scientific goals. The original experiment plan was:

The experimental part of the Phase II of the experiment was completed in October 2012. We completed the experiment with 45 and 122 kg explosions.

EXPERIMENT LOCATION OVERVIEW

To conduct the proposed series of fracture-decoupled explosions, we have chosen a site on private land near Groton, New Hampshire. The major rock type at the site is Kinsman Granodiorite created during late stages of the Acadian orogeny (400 – 390 ma) (Allen, 2003). Gravity studies (e.g. Smith, 2009) indicate that the Kinsman Granodiorite is a 2 to 3 kilometer-thick sill, rather than a batholith with deep roots. There is some debate about whether the Kinsman rocks originated solely as a result of melting of the enclosing metasediments**,** or whether they received input from a mantle source (Lyons, 1988; Rodgers, 1970). Later more volatile and less viscous portions of the melt were forced into the surrounding rock to slowly cool and form Newfound Lake area pegmatites, characterized by the very large mineral size.

Large crystals of mica and feldspar deposits found in pegmatites were extensively mined in the area and supported the local economy from the early 1800s to the middle 1900s (e.g. Cameron et al., 1954).

Several outcrops have been found on or near the road, which in this area appears to have very thin sediment layer. The topsoil layer at the site is approximately 0.5 m thick on the ridges, and becomes 1-2 m around the stream valleys. The drilling has shown that it varied between 0 and 2 m at the test site.

EXPLOSIONS

Three pairs of explosions were detonated to examine fracture decoupling. The first shot of each pair was detonated in virgin rock and the second was detonated in the rock fractured/damaged by the first explosion. This procedure was performed for two 45 kg ammonium nitrate fuel oil (ANFO) explosions, two 45 kg Composition B (Comp B) explosions, and two 122 kg of ANFO explosions.

To conduct the blasts, 23 cm diameter holes were drilled to depths between 16 and 19 m. The holes were then loaded with explosive and back-filled with ¾" stemming (small rock pieces used to fill up the loaded borehole). After detonation of the virgin rock shot, boreholes were drilled in close proximity to the original hole down into the damage zone. The follow-up explosions were then conducted in the same manner. The 122 kg ANFO shot ejected all the stemming without damaging the borehole, so a new hole did not need to be drilled. A cavity at the bottom of the hole was noted during loading of the second shot.

An additional explosion was conducted at the Decoupling 2011 test site 150 meters to the SSW as a comparison to the previous experiment. This explosion consisted of 45 kg of ANFO. Table 1 lists the experiment explosion characteristics.

Table 1. Explosion locations and origin times.

Shot	Date	Time	Lat	Lon	Elev (m)	Centroid Depth (m)	Charge Size (kg)	Description
FD12	10/5/2012	20:50:17.356	43.68844	-71.85069	393.53	16.15	45.36	ANFO
FD13	10/5/2012	21:12:25.127	43.68840	-71.85100	394.00	16.92	45.36	Comp B
FD11	10/5/2012	21:40:15.249	43.68826	-71.85080	394.39	16.46	122.47	ANFO
FD22	10/19/2012	17:02:12.069	43.68843	-71.85071	393.53	17.07	45.36	ANFO reshoot
FD23	10/19/2012	17:18:15.075	43.68841	-71.85098	393.44	17.37	45.36	Comp B reshoot
FD21	10/19/2012	17:41:16.864	43.68826	-71.85080	394.39	16.92	122.47	ANFO reshoot
FDOS	10/19/2012	18:03:57.481	43.68713	-71.85134	384.05	14.94	45.36	ANFO old test site reshoot

SEISMIC INSTRUMENTATION

WGC deployed 30 local distance (600 m to 10 km) short-period seismometers. These instruments consisted of L-22 and L-4C 3D seismometers installed to achieve distance and azimuthal coverage for the explosions (Figures 1 and 2). We installed five profiles along the existing roads or trails extending in approximately north (N profile), northeast (NE profile), east (E profile), south (S profile), and west (W profile) directions. Reftek RT130 digitizers recorded these sensors at 1000 samples per second (sps) and a gain of 1 for the stations comprising the close-in (near) linear arrays (all 3C stations shown in Figure 2 except NNE3B). The stations at greater distance were recorded at 500 sps and a gain of 32. Table 2 lists the three-component locations.

To reduce the close-in sensor distance spacing, vertical component Reftek RT125 (“Texan”) recorders with 4.5 Hz geophones were deployed in arrays extending up to 2 km away from the test site (Figure 2). These sensors were recorded at 1000 sps with a gain of 32. Table 3 lists the RT125 locations. All RT125 recorders were deployed for the virgin rock explosions, but only a subset of RT125 recorders were deployed for the reshoot explosions.

Figure 1. Three-component stations (red pins) and explosion locations (flames). Google Earth map.

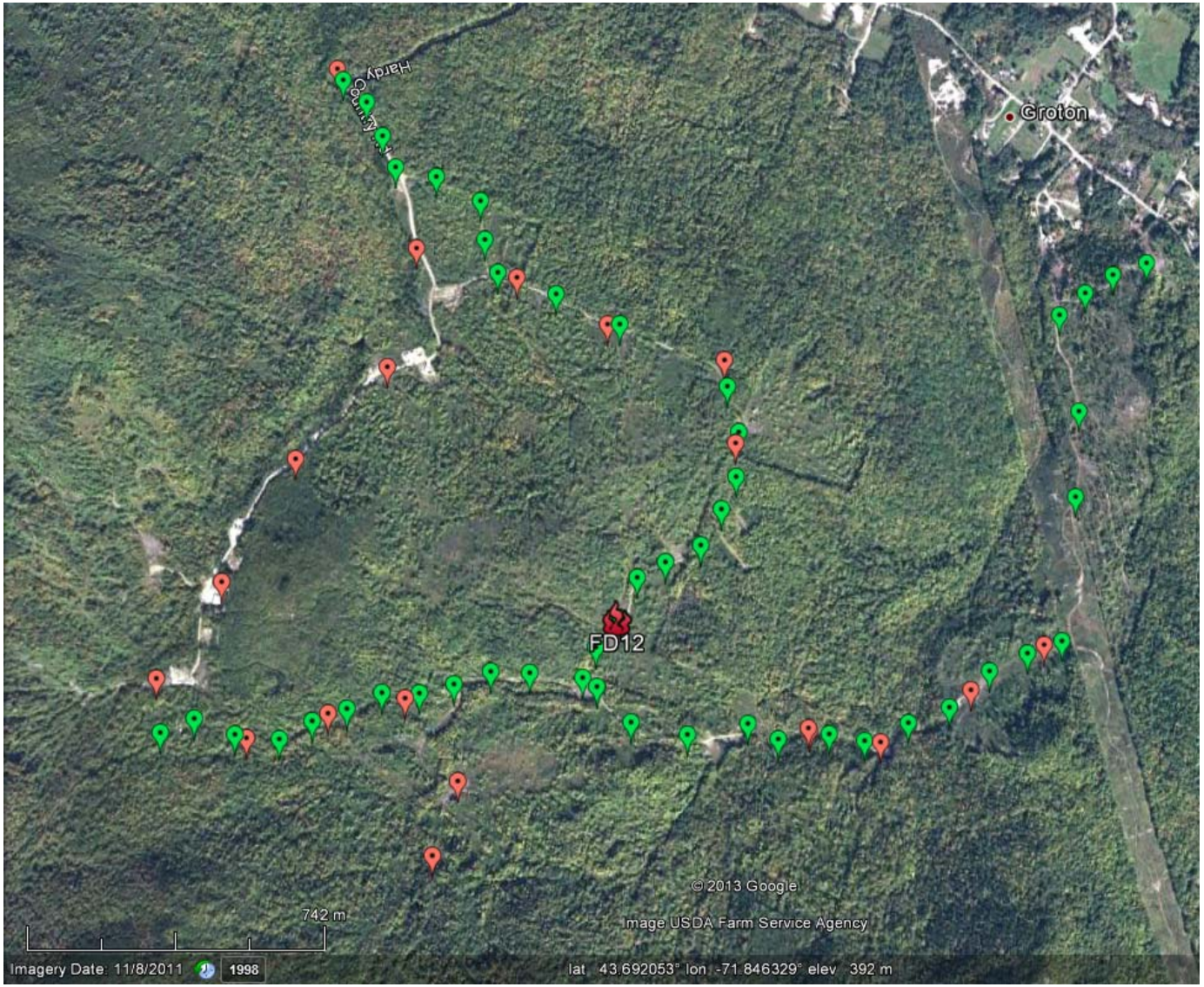

Figure 2. Close-in three-component stations (red pins), RT-125 Texans (green pins), and explosion locations (flames). Google Earth map.

Table 2. Three-component seismic stations.

Station	Lat	Lon	Elev (m)	DAS	Sensor	Gain	Sample Rate
ESE2	43.68598	-71.84411	348	964E	L22	1	1000
ESE3	43.68562	-71.84161	346	9E39	L22	1	1000
ESE4	43.68696	-71.83847	360	A095	L22	1	1000
ESE5	43.68805	-71.83595	363	98AA	L22	1	1000
NNE2	43.69308	-71.84662	400	A203	L22	1	1000
NNE3A	43.69513	-71.847	394	9BBB	L22	1	1000
NNE3B	43.69513	-71.847	394	9668	L22	32	1000
NNN3	43.69603	-71.85101	375	AB17	L22	1	1000
NNW4	43.69722	-71.85416	364	AB07	L22	1	1000
NNW5	43.69798	-71.85768	350	9DDF	L22	1	1000
NNW6	43.70261	-71.86061	308	9754	L22	1	1000
SSW2	43.68479	-71.85603	420	98EA	L22	1	1000
SSW3	43.68305	-71.85679	458	9AB5	L22	1	1000
NWN4	43.69498	-71.85859	380	9395	L22	1	1000
WNW4	43.69269	-71.86165	397	AB1B	L22	1	1000
WSW2	43.68682	-71.85782	423	969F	L22	1	1000
WSW3	43.68646	-71.8604	425	9DB4	L22	1	1000
WSW4	43.68587	-71.86312	462	939F	L22	1	1000
WSW5	43.68732	-71.86617	435	9BC4	L22	1	1000
WWW4	43.68967	-71.86404	404	9407	L22	1	1000
CHCK	43.7469	-71.85748	453	965F	L-4C 3D	32	500
GROT	43.69747	-71.83315	259	9389	L22	32	500
KILL	43.67419	-71.80583	354	9D7C/9DAA	L-4C 3D	32	500
ORAN	43.69027	-71.88821	432	9AB0	L-4C 3D	32	500
ALAN	43.71722	-71.77954	250	9E3A	L-4C 3D	32	500
HECK	43.73188	-71.92506	410	A125	L-4C 3D	32	500
CHET	43.60531	-71.87672	569	91E6	L-4C 3D	32	500
CAPS	43.64738	-71.74759	228	AAEB	L-4C 3D	32	500
CARD	43.66697	-71.93842	591	9E00	L-4C 3D	32	500
WELF	43.66142	-71.87376	432	967D	L-4C 3D	32	500

Table 3. RT125 vertical component seismic stations.

Station	Lat	Lon	Elev (m)	DAS	Sensor	Gain	Sample Rate
TE02	43.68706	-71.85136	396	2628/1798	4.5 Hz geophone	32	1000
TE03	43.68619	-71.85019	399	3666/3624	4.5 Hz geophone	32	1000
TE04	43.68587	-71.84827	384	4004/2889	4.5 Hz geophone	32	1000
TE05	43.68610	-71.84620	358	2603/2164	4.5 Hz geophone	32	1000
TE06	43.68571	-71.84515	356	3880/2915	4.5 Hz geophone	32	1000
TE07	43.68583	-71.84339	357	1916/3733	4.5 Hz geophone	32	1000
TE08	43.68565	-71.84216	343	3737/2668	4.5 Hz geophone	32	1000
TE09	43.68609	-71.84064	357	2743	4.5 Hz geophone	32	1000
TE10	43.68649	-71.83923	363	3985	4.5 Hz geophone	32	1000
TE11	43.68740	-71.83785	358	4084	4.5 Hz geophone	32	1000
TE12	43.68784	-71.83653	347	3668	4.5 Hz geophone	32	1000
TE13	43.68814	-71.83532	338	2673	4.5 Hz geophone	32	1000
TE14	43.69175	-71.83475	211	2949	4.5 Hz geophone	32	1000
TE15	43.69392	-71.83457	289	3681	4.5 Hz geophone	32	1000
TE16	43.69641	-71.83514	270	3966	4.5 Hz geophone	32	1000
TE17	43.69698	-71.83421	251	3784	4.5 Hz geophone	32	1000
TE18	43.69747	-71.83318	246	3898	4.5 Hz geophone	32	1000
TE19	43.69780	-71.83192	242	2502	4.5 Hz geophone	32	1000
TN01	43.68875	-71.85055	403	2710/3598	4.5 Hz geophone	32	1000
TN02	43.68976	-71.84998	402	2126/2006	4.5 Hz geophone	32	1000
TN03	43.69014	-71.84902	399	3744/3988	4.5 Hz geophone	32	1000
TN04	43.69056	-71.84781	406	3706/3713	4.5 Hz geophone	32	1000
TN05	43.69145	-71.84710	413	2479/2419	4.5 Hz geophone	32	1000
TN06	43.68836	-71.85127	393.529	3677/4036	4.5 Hz geophone	32	1000
TN07	43.69335	-71.84651	409	2634/2479	4.5 Hz geophone	32	1000
TN08	43.69448	-71.84690	406	2889/2699	4.5 Hz geophone	32	1000
TN09	43.69603	-71.85059	385	4036/2100	4.5 Hz geophone	32	1000
TN10	43.69679	-71.85279	374	2100/2888	4.5 Hz geophone	32	1000
TN11	43.69735	-71.85483	366	2699/3746	4.5 Hz geophone	32	1000
TN12	43.69818	-71.85529	348	2888	4.5 Hz geophone	32	1000
TN13	43.69917	-71.85547	351	3935	4.5 Hz geophone	32	1000
TN14	43.69979	-71.85702	348	3733	4.5 Hz geophone	32	1000
TN15	43.70004	-71.85845	341	2668	4.5 Hz geophone	32	1000
TN16	43.70085	-71.85894	345	1836	4.5 Hz geophone	32	1000
TN17	43.70173	-71.85953	336	3746	4.5 Hz geophone	32	1000
TN18	43.70231	-71.86038	319	3908	4.5 Hz geophone	32	1000

Station	Lat	Lon	Elev (m)	DAS	Sensor	Gain	Sample Rate
TW01	43.68804	-71.85139	415	2565/1676	4.5 Hz geophone	32	1000
TW02	43.68728	-71.85185	393	3598/2170	4.5 Hz geophone	32	1000
TW03	43.68742	-71.85363	409	2505/3706	4.5 Hz geophone	32	1000
TW04	43.68746	-71.85494	409	3988/2565	4.5 Hz geophone	32	1000
TW05	43.68715	-71.85619	417	2170/1678	4.5 Hz geophone	32	1000
TW06	43.68694	-71.85734	421	1676	4.5 Hz geophone	32	1000
TW07	43.68696	-71.85859	427	2164	4.5 Hz geophone	32	1000
TW08	43.68657	-71.85977	427	2006	4.5 Hz geophone	32	1000
TW09	43.68627	-71.86094	432	2419	4.5 Hz geophone	32	1000
TW10	43.68583	-71.86205	439	3624	4.5 Hz geophone	32	1000
TW11	43.68596	-71.86350	438	1798	4.5 Hz geophone	32	1000
TW12	43.68636	-71.86483	453	2915	4.5 Hz geophone	32	1000
TW13	43.68604	-71.86590	464	1678	4.5 Hz geophone	32	1000

CONCLUSIONS

The Phase II experiment was conducted in order to verify the repeatability of the seismic observations (amplitude reduction) using explosions of different yields and possibly different explosive types. The second shot of the Phase I experiment was conducted in the rubble zone of a larger explosion, which produced more significant damage to the subsurface than would have been produced by the same yield explosion. During Phase II we detonated 3 pairs of co-located explosions. Both explosions in each pair were of the same yield. The fracture zones produced by the first explosions were less extensive than the fracture zone from Phase I first explosion. Therefore the amplitude reduction was less significant for the Phase II explosions (on average 1.07 and 1.25 respectively, or 7% and 20% amplitude reduction) compared to the ratios between the Phase I explosions (on average 2.25 or 56% amplitude reduction).

Spectral analysis of the seismic records shows that fractured media reduces the corner frequency; however the frequency roll-off remains approximately the same as for the explosion in the undamaged rocks.

The amplitude reduction effect was likely inhibited by water saturation of the emplacement media. One of the potential research directions is to examine the differences in seismic radiation between repeat explosions in dry and saturated rocks. We will try to address this issue during our upcoming 2013 field campaign.

ACKNOWLEDGEMENTS

This research was sponsored by DTRA grant HDTRA1-11-1-0029. We would like to thank our field crew including Aaron Ferris, Noel Barstow, Pnina Miller, and Christopher Sanborn. We thank IRIS PASSCAL for providing sensors and systems for this project.

REFERENCES

Allen, T. (2003) “Bedrock Geology of the Lake Sunapee Area, West-Central New Hampshire”; Guidebook of the 95th Annual New England Intercollegiate Geological Conference (NEIGC), Trip A4

Cameron, E., Larrabee, D., McNair, A., Page, J., Stewart, G., and Shainin, V. (1954). Pegmatite Investigations 1942-1945 New England; Geological Survey Professional Paper 255, US Government Printing Office

Knowles, C. (2006). Omega test series, Technical report to Defense Threat Reduction Agency, DTRA 01-99-D-0047, October 2006.

Lyons, J. (1988). Geology of the Penacook and Mt. Kearsarge Quadrangles, New Hampshire; Guidebook of the 80th Annual NEIGC, Trip A4

Lyons, J., Bothner, W., Moench, R., and Thompson, J.B. Jr. (1997). Bedrock Geologic Map of New Hampshire; US Geological Survey, scale 1:250,000

Rodgers, J. (1970) “The Tectonics of the Appalachians”; John Wiley & Sons, Inc.

Sokolova, I. N. (2008). Investigation of dynamic parameters of seismic records of initial and repeated explosions, (*in Russian*), *NNC RK Bulletin*, **33**(1), 68-73.

Stroujkova, A., J. Bonner, and T. Rath (2012). Effect of fractures on seismic amplitudes from explosions, *Bull. Seism. Soc. Am*. in press.

Van Diver, B. (1987). Roadside Geology of Vermont and New Hampshire, *Mountain Press Publishing Co*.